



# Characterization and mode of occurrence of rare earth elements and yttrium in fly and bottom ash from coal-fired power plants in Java, Indonesia

Dea Anisa Ayu Besari<sup>1</sup> · Ferian Anggara<sup>2,3</sup> · Widya Rosita<sup>3,4</sup> · Himawan T. B. M. Petrus<sup>3,5</sup>

Received: 28 April 2021 / Accepted: 17 January 2022  
© The Author(s) 2022

## Abstract

Fly and bottom ash (FABA) produced primarily from coal combustion in a coal-fired power plant consists of fine particles of the organic and inorganic mixture and trace elements. Eight FABA samples from coal-fired power plants in Java, Indonesia, had been collected for composition and rare earth element and Yttrium (REY) mode of occurrence identification. The geochemical composition of both major and trace elements was determined by inductively coupled plasma-mass spectrometry/atomic emission spectrometry (ICP-MS/AES). Furthermore, the composition of FABA was identified by petrography with reflected light microscopy and X-ray diffraction (XRD) analysis. Simultaneously, scanning electron microscope determines the mode of occurrence of REY with an energy-dispersive X-ray (SEM-EDX). The study finds that the inorganic component of FABA consists of glass, Fe–Mg spinel, mullite, quartz, Fe-oxide mineral, and K-feldspar. In contrast, the organic component is dominated by unburned coal. Glass is the most abundant component with cenospheres as major and pleiospheres as minor constituents. Trace elements analysis indicates REY concentration with heavy REY (HREY) distribution pattern. Moreover, SEM-EDX analysis results show that Yttrium (Y) occurs in glass and has a low concentration in spinel. From the mode occurrence of REY, in particular Yttrium, it can be predicted that alkaline fusion followed by acid leaching will be the most appropriate extraction method to extract REY from Indonesian FABA.

**Keywords** REY · Fly ash · Bottom ash · Glass · Indonesia

✉ Ferian Anggara  
ferian@ugm.ac.id

- <sup>1</sup> Department of Geological Engineering, Graduate School of Geological Engineering, Universitas Gadjah Mada, Jalan Grafika No. 2 Kampus UGM Bulaksumur, D.I. Yogyakarta 55281, Indonesia
- <sup>2</sup> Department of Geological Engineering, Faculty of Engineering, Universitas Gadjah Mada, Jalan Grafika No. 2 Kampus UGM Bulaksumur, D.I. Yogyakarta 55281, Indonesia
- <sup>3</sup> Unconventional Geo-Resources Research Group, Faculty of Engineering, Universitas Gadjah Mada, Jalan Grafika No. 2 Kampus UGM Bulaksumur, D.I. Yogyakarta 55281, Indonesia
- <sup>4</sup> Department of Nuclear Engineering and Engineering Physics, Faculty of Engineering, Universitas Gadjah Mada, Jalan Grafika No. 2 Kampus UGM Bulaksumur, D.I. Yogyakarta 55281, Indonesia
- <sup>5</sup> Department of Chemical Engineering, Faculty of Engineering, Universitas Gadjah Mada, Jalan Grafika No. 2 Kampus UGM Bulaksumur, D.I. Yogyakarta 55281, Indonesia

## 1 Introduction

Particulate Indonesia's energy demand is dominated by electricity consumption and is expected to increase dramatically, driven by economic development and the fast-growing population. The Indonesian government has set the target for electricity generation up to 135.5 GW by 2025 to balance this energy demand and laid out in Presidential Regulation (PerPres) No.22/2017. The primary energy supply in Indonesia is mainly based on fossil fuels like oil, gas, and coal. National energy policy setting a target energy mix in the year 2025 will be oil (20%), gas (30%), coal (33%), and new and renewable energy (17%), as can be seen in Fig. 1. As for coal consumption, the power plant sector is the biggest consumer in Indonesia. A significant increase in coal consumption in the power plants sector from 56 mt in 2006 to 123.2 mt in 2025 will produce 11.38 mt of FABA in coal-fired power plants. FABA is a hazardous solid waste and toxic category in which the toxic elements might affect all beings (plant, animal, and human) (Bashkin et al. 2002; Dai et al. 2005). In

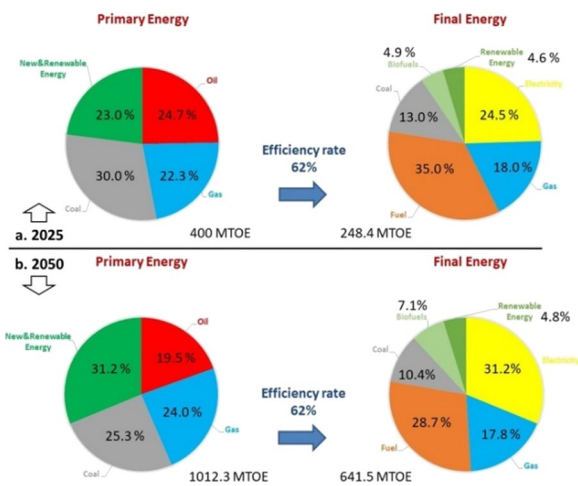


**Fig. 1** The target of Indonesian energy mixed in 2025 (a top) and 2050 (b bottom) based on Presidential Regulation No. 22 of 2017. Coal is still the main primary energy until 2025 and 2050 to produce electricity as final energy up to 135.5 GW and 443.1 GW in 2025 and 2050

Indonesia, FABA has many requirements for treatment and many permits that must be executed (storage clearance, collecting, transportation license, utilization permit, and landfill permit) (Indonesia Government Regulation No. 101/2014).

Faced with a large amount of FABA resulting from coal-fired power plant production, the disposal will be a major issue due to its necessity of land occupancy. To eliminate this problem, FABA utilization has been proposed from cement, concrete, structural fill (Duminda et al. 2014), soil stabilization, and agriculture (Yao et al. 2015) to the recovery of valuable matters such as cenospheres (Hirajima et al. 2008, 2010; Petrus et al. 2011) as well as valuable elements (Dai and Finkelman 2018). Another reuse option for commercial applications of coal ash (FABA) is its rare earth elements and yttrium (REY) content and the potential for it to be extracted (Seredin and Dai 2012; Blissett et al. 2014). Scandium (Sc) and yttrium (Y), with chemical similarity to the lanthanides, are typically included in the rare earth elements classification (Pecht et al. 2012). The essential commercial usage of REY drives the increasing needs for REY for electronic and optical industries, oil extraction and refining, automobile industries, information and nanotechnologies, nuclear reactors, and green energy developments (Seredin and Dai 2012). According to their study, it was found that the average of REY contents in the world (404 ppm) and USA (517 ppm) coal ashes are approximately three times higher than in the upper continental crust (UCC). Meanwhile, there has been no research in Indonesia regarding the reuse options of FABA as alternative sources of REY (Anggara et al. 2018, 2019, 2020; Besari 2018) To provide a comprehensive database on REY potential in coal seams and FABA from coal-fired power plants in Indonesia, a study

on the composition and mode of occurrence of REY in coal and FABA has been conducted.

Determining the mode of occurrence is essential to distinguish the appropriate processing technique needed to extract the REY. There are two limiting techniques applied in REY extraction from coal fly ash, acid leaching and alkaline-acid leaching (Zhang et al. 2020; Rybak and Rybak 2021), although there are several approaches applied prior to those aforementioned techniques to improve the leachability of REY from coal fly ash. For REY in the lignite, which is associated with complexed organic acids, can be extracted with mild acidic condition using 0.5 M of  $H_2SO_4$  with recovery of about 90% (Laudal et al. 2018). In the case of bituminous coals, comprehensive approaches based on acid leaching have been conducted with recovery higher than 80% (Honaker et al. 2017; Zhang et al. 2018, 2020). Other studies on REY associated with magnetic coal fly ash and or Fe and Ca enriched fraction can be successfully extracted using acid leaching (King et al. 2018; Taggart et al. 2018; Prihutami et al. 2021). However, it has also been reported that REY is associated with aluminosilicates (Kolker et al. 2017; Hower et al. 2018). The association with aluminosilicate renders the REY extraction using acid leaching. Destruction of the aluminosilicate structure using alkaline followed by acid leaching has resulted in higher recovery of REY (King et al. 2018; Taggart et al. 2018; Manurung et al. 2020).

Thus, being able to establish the comprehensive database on REY in coal seams and FABA and their mode of occurrence will surely beneficial to predict the most appropriate technique to extract.

## 2 Experiments

### 2.1 Materials

Coal, FA, and BA samples were collected from eight coal-fired power plants in the northern part of Java, Indonesia (Fig. 2). All coal-fired power plants in this study were used pulverized coal combustion types. The boiler temperature from each power plant ranged from 1100–1400 °C. Each of the FA and BA samples was collected from the disposal of the Electrostatic Precipitator (ESP) unit as much as 25 kg. Each of the FA and BA samples collected from each power plant came from the same feed coal (Table 1) and the same operational condition. This can be considered that each sample is representative enough.

### 2.2 Experimental methods

The feed coal of Paiton 1, Paiton 2, and Tanjung Jati power plants are sub-bituminous coal from some coal basins in



**Fig. 2** Location of eight coal-fired power plants in northern Java, Indonesia. Coal and FABA samples were taken from the power plants (Map data: Google, accessed 14 February 2022)

**Table 1** List of samples collected from 8 power plants in Java, Indonesia

Power plant location	Sample		
	Feed coal	Fly ash	Bottom ash
Paiton 2	C-1	FA-1	BA-1
Paiton 1	C-2	FA-2	BA-2
Pacitan	C-3	FA-3	BA-3
Tuban	C-4	FA-4	BA-4
Indramayu	C-5	FA-5	BA-5
Rembang	C-6	FA-6	BA-6
Ubjom Paiton	C-7	FA-7	BA-7
Tanjung Jati	C-8	FA-8	BA-8

Kalimantan. The feed coal of Pacitan, Rembang, and Indramayu power plants comprise sub-bituminous coal from Kalimantan and South Sumatra Basin. While feed coal of the Indramayu power plant is from the South Sumatra Basin. To be able to provide comprehensive information for further utilization on REY possible extraction, several analytical approaches have been conducted, as follows:

(1) Proximate analysis.

To evaluate the ash yield of the coal, this analysis was conducted according to ASTM D-3174.

(2) Petrography analysis of the coal and FABA.

A polished block of coal and FABA samples were prepared using Specifix-20 Kit and Struers Labo System. Coal petrography was done according to ASTM D2799-05a, and maceral classification followed the ICCP System 1994 (Pickel et al. 2017; Sýkorová et al. 2005; ICCP 2001). Identification of the abundance of the organic and inorganic composition of FABA is using genetic classification (Hower 2012).

(3) Mineralogy analysis.

Analysis using XRD with the bulk method with  $2\theta$  from  $2^\circ$  to  $60^\circ$  was conducted in the analytical laboratory of the Department of Geological Engineering, Universitas Gadjah Mada. The analysis was performed on fly ash samples to observe the mineral content in fly ash that cannot be examined in the petrographic analysis, including the mineralogical changes due to the coal burning in the power plant. Mineralogy of fly ash is crucial to justify the REY mode of occurrence (Dai et al. 2012).

(4) Geochemistry analysis.

For all samples, major and trace element was determined using ICP-AES and ICP-MS in the ALS Geochemistry Laboratory, Kamloops, Canada using the fused bead method before acid digestion. REY mode of occurrence was observed using SEM-EDX in the Laboratorium Teknologi Mineral dan Batubara (TEKMIRA), Bandung, Indonesia, for selected samples regarding the abundance of REY.

### 3 Results and discussion

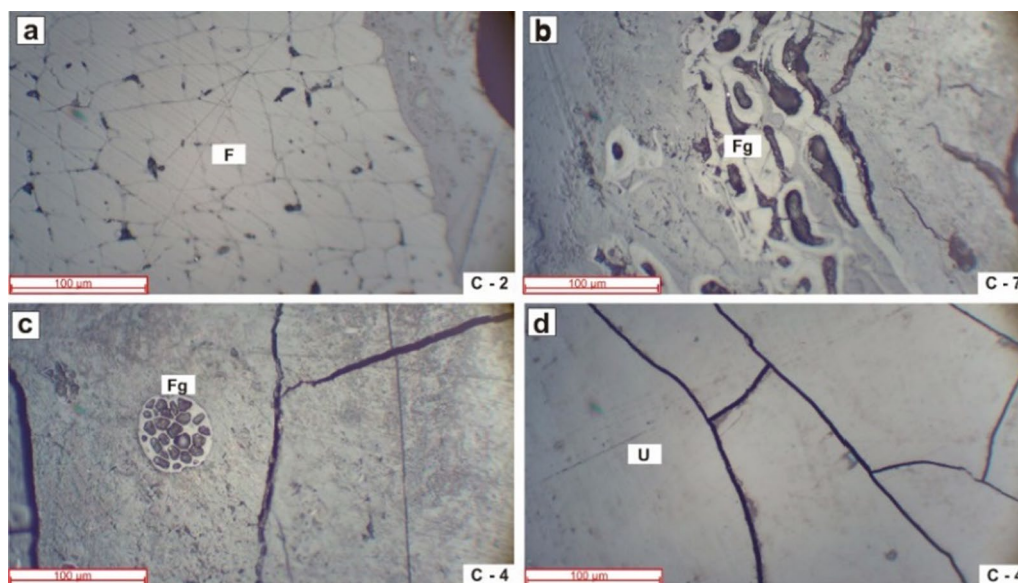
#### 3.1 Coal characteristics

As shown in Table 2, feed coal from 8 power plants in Java indicate average value of ash yield ranging 3.27–5.34 wt%. The average moisture content ranged from 19.5 to 34.39 wt%. The average volatile matter ranged from 38.56 to 43.82 wt%. The average fixed carbon contents ranging from 35.02 to 42.15 wt%. The average calorific value range from 4240 to 5820 kcal/kg. The average sulfur content varies between 0.23 and 79 wt%.

Results of coal petrography analysis revealed that coal samples are rich in huminite in the range of 66%–78%. Ulminite is the most common telohuminite maceral subgroup

**Table 2** Proximate analyses (wt%) and calorific value (kcal/kg) of feed coals from 8 power plants in Java, Indonesia

Sample	M	A	VM	FC	S	CV
C-1	34.39	3.27	38.56	35.02	0.23	4240
C-2	34.39	3.62	38.56	35.02	0.23	4240
C-3	30.43	3.81	39.42	40.57	0.26	5693
C-4	30.36	5.34	43.82	40.57	0.42	5820
C-5		5.23				
C-6	31.98	5.1	42.44	38.18	0.3	5609
C-7		3.59			0.3	
C-8	19.59	4.94	40.91	42.15	0.79	5584

**Fig. 3** Macerals in coal samples. **(a)** Fusinite (F); **(b)** Funginite (Fg) in sample C-7; **(c)** Funginite (Fg) in sample C-4; and **(d)** Ulminite (U); All photomicrographs are taken under white light**Table 3** Petrographic analysis and ash yield of coal samples

Sample	Huminite (%)	Liptinite (%)	Inertinite (%)	Mineral matter (%)	Ash yield (wt%)
C-1	76	7	14	3	3.27
C-2	71	8	15	6	3.62
C-3	78	4	16	5	3.81
C-4	66	8	19	7	5.34
C-5	70	6	17	7	5.23
C-6	67	9	18	6	5.10
C-7	75	8	13	4	3.59
C-8	73	5	17	5	4.94

and is present in all coal samples. The content varies from 13% to 19% in inertinite and is mainly presented as semi-fusinite and funginite (Fig. 3). While liptinite content is in the range of 4%–9%, suberinite, sporinite, and liptodetrinite are the most common liptinite-group macerals observed.

The detailed composition of the maceral content, minerals matter, and ash yield of coal samples are presented in Table 3. In general, ash yield will be associated with FABA resulting from a coal-fired power plant affected by the coal's certain maceral and mineral content. As it can be

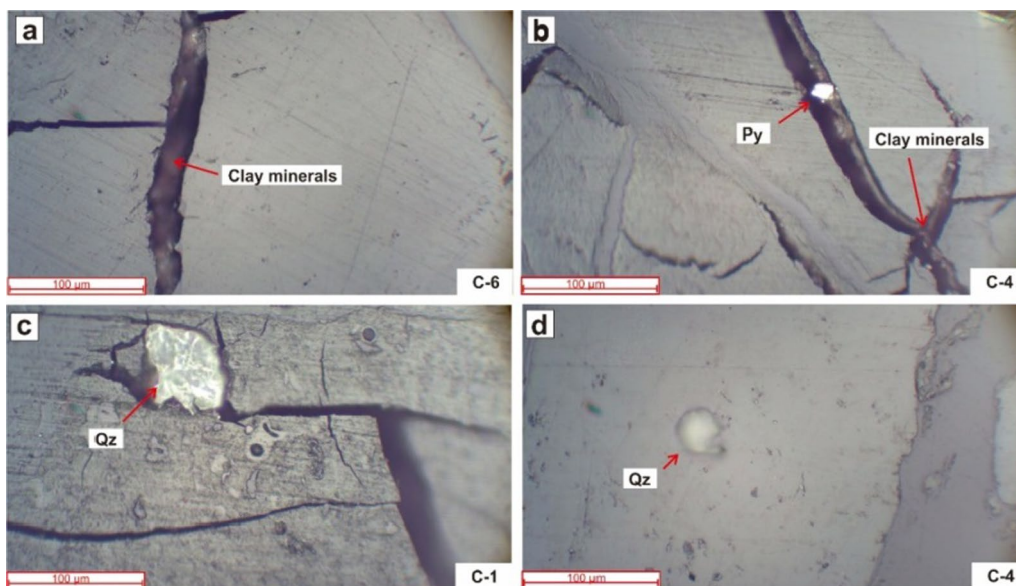


**Fig. 4** Mineral matter in coal samples. (Clay minerals, pyrite (Py), and quartz (Qz); All photomicrographs are taken under white light)

seen from Table 3, the ash yield in the concentration range of 3.27%–5.34% possesses an inline correlation with the inertinite and minerals matter in the coal. The higher inertinite and minerals matter in the coal, the higher the ash yield.

Instead of a detailed depiction of the maceral in the coal samples, the mineral matter can also be determined from the petrographic analysis. It can be observed that the minerals matter are mainly contained clay minerals, quartz, and pyrite (Fig. 4). Clay minerals dominate the proportion of minerals in the concentration range of 33.3%–66.77%, followed by pyrite and quartz in the same concentration range of 16.7%–33.3% (Fig. 5). The petrographic analysis on minerals matter follows the major oxides observed in coal samples

dominated by SiO<sub>2</sub>, Al<sub>2</sub>O<sub>3</sub>, and Fe<sub>2</sub>O<sub>3</sub> (“Appendix”) as the components of clay minerals, quartz, and pyrite.

### 3.2 FABAs organic composition

The FABAs components can be grouped into two broad categories; organic and inorganic. The organic component of FABAs consists of unburned coal (UC). Occasionally, UC attaches to and binds together with crystalline minerals or amorphous glass. UC can be used as an indicator of inefficiencies in coal combustion. The nature and proportions of the macerals in feed coal significantly affected the UC content in FABAs. Inertinite-group macerals are more resistant

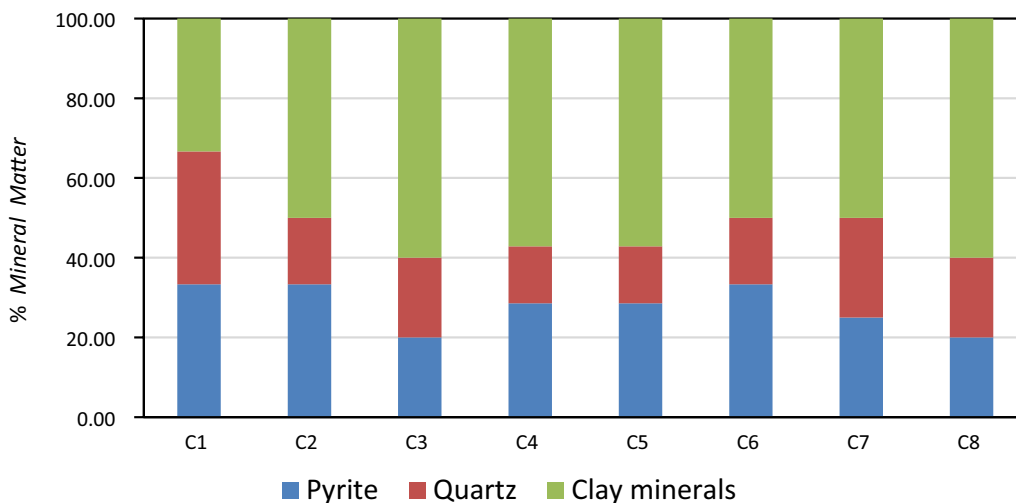


**Fig. 5** Percentage mineral matter in coal samples (normalized to 100%)

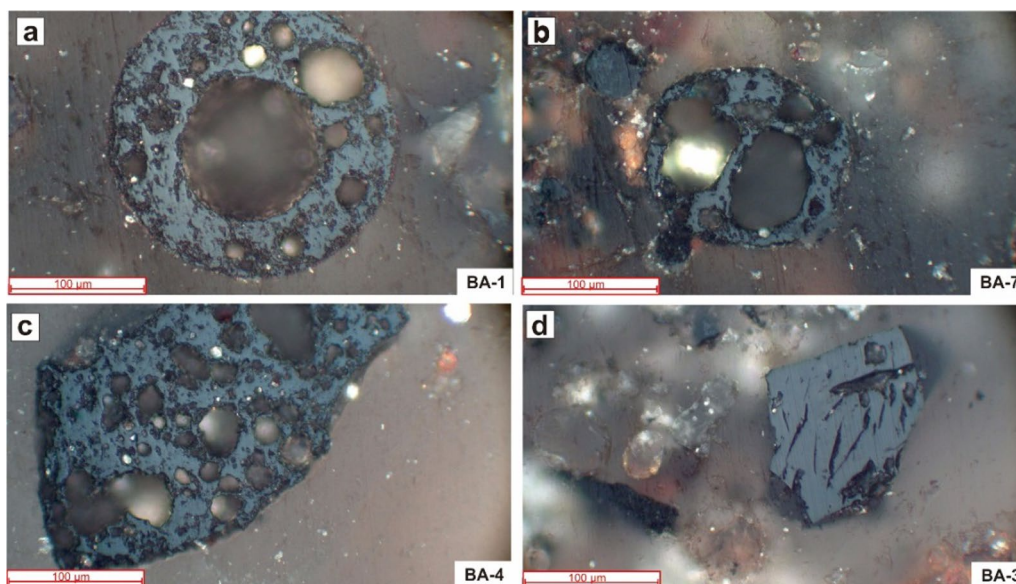


**Fig. 6** Unburned coals: **a** crassisphere; **b** tenuisphere; **c** crassinetwork; **d** solid. (All photomicrographs are taken under white light)

to combustion than other macerals (Hower et al. 2017). UC was observed in both fly and bottom ash (FABA) from the petrographic analysis, as shown in Fig. 6. The textured form of UC in FABA was observed as tenuisphere, crassisphere, crassinetwork, and solid with an abundance of about 7.4%–12.4% in FA and 16%–29.6% in BA (Tables 4 and 5). UC concentration in FABA is strongly affected by inertinite content in coal (13%–19%, Table 3), which is relatively difficult to burn compared to vitrinite and huminite (Hower et al. 2017).

### 3.3 FABA inorganic composition

As observed from the petrographic analysis, inorganic components of FABA consist of glass, mullite, Fe-oxide minerals, quartz, and spinel (Fig. 7). The mineralogical compositions identified by XRD show the existence of quartz, mullite, k-feldspar, hematite, magnetite, Fe-spinel, and Mg-spinel. It was found that there is varied mineralogy in terms of Fe-oxide mineral and spinel due to the limitation of the petrographic analysis. The Fe-oxide minerals in FA

**Table 4** Percentage of organic and inorganic components of fly ash (FA) samples based on petrographic and XRD analysis

Item	FA-1	FA-2	FA-3	FA-4	FA-5	FA-6	FA-7	FA-8
<i>Petrographic analysis</i>								
Quartz (%)	14.4	13.8	13.5	14.2	15.3	15.8	12.4	16.7
Mullite (%)	14.4	13.5	12.5	13.6	12.7	11.6	11.6	14.5
Fe-oxide mineral (%)	11.8	9.3	10.5	9.5	11.8	9.5	14.2	8.4
Spinel (%)	8.4	11.6	10.7	5.8	6.0	12.7	16.7	8.5
Glass (%)	38.7	40.2	35.6	42.7	41.5	38.7	33.5	37.8
Unburned carbon (%)	12.4	11.6	17.1	14.2	12.7	11.6	11.6	14.0
K-feldspar (%)	–	–	–	–	–	–	–	–
<i>XRD analysis</i>								
Quartz (%)	70.1	56.3	57.6	53.5	44.6	42.4	37.4	52.9
Mullite (%)	18.3	21.8	12.4	31.6	15.8	12.1	17.1	6.4
Hematite (%)	7.7	12.1	15.8	5.3	19.4	18.0	–	12.2
Magnetite (%)	–	–	9.0	5.1	–	–	29.6	–
Fe-spinel (%)	–	–	–	–	–	20.5	–	18.2
Mg-spinel (%)	3.9	11.5	2.9	4.5	15.7	7.1	16.6	10.4
Glass (%)	–	–	–	–	–	–	–	–
Unburned carbon (%)	–	–	–	–	–	–	–	–
K-Feldspar (%)	–	7.7	–	–	4.6	–	–	–

**Table 5** Percentage of organic and inorganic components of BA samples based on petrographic analysis

Sample	Unburned coal (%)	Glass (%)	Quartz (%)	Fe-oxide minerals (%)	Spinel (%)	Mullite (%)
BA-1	16.0	37.5	13.8	16.4	8.5	7.8
BA-2	18.7	36.5	13.6	14.4	10.2	6.5
BA-3	18.2	35.6	12.4	12.7	15.1	6.2
BA-4	17.6	39.6	14.4	9.1	11.1	8.2
BA-5	19.3	38.9	13.8	8.5	11.8	7.6
BA-6	17.6	36.2	14.5	10.0	15.3	6.4
BA-7	18.5	34.7	14.5	10.2	15.3	6.7
BA-8	18.7	35.6	16.2	9.6	12.4	7.5

samples are dominated by hematite, while the magnetite is rarely found. As for spinels, it was detected in two types and identified as Mg-spinel and Fe-spinel. The Fe-spinel is identified only in two samples of FA (FA-6 and FA-8). Furthermore, the compositions of FA and BA are presented in Tables 4 and 5.

#### (1) Glass.

The glass is composed of the transformation of clay minerals during coal combustion. This study found that clay minerals are the most abundant mineral matter found in all coal samples (Fig. 5). Thus, glass dominates the inorganic matter of FABA with a composition of about 33.5%–42.7% in FA and 34.7%–39.6% in BA. With a chemical composition of silica dioxide, glass has an amorphous structure. From the petrographic analysis, Glass in FABA can be found in the form of cenospheres and pleiospheres, as seen in Fig. 7. Cenospheres are characterized by rounded hollow glass spheres and are mostly presented in a significant quantity (up to 92.3% in FA). Meanwhile, pleiospheres occur as multiple hollow glass spheres which are not perfectly rounded.

#### (2) Quartz.

In the crystalline structure, Quartz in FABA originally comes from its coal (Dai et al. 2010). Due to its stability to high temperature with a melting point of about 1700 °C, quartz will remain in its form when the boiler temperature is only at the temperature of 1400–1500 °C (Hower 2012). Besides glass, quartz is also the major mineral found in FABA, with 12.4%–17.1% in FA and 7.1%–16.2% in BA. As shown in Fig. 7, quartz is characterized as a colorless to white spectrum with angular-subrounded morphology.

#### (3) Mullite.

Other crystalline minerals observed in these FABA samples (Fig. 7) were mullite with a composition of 6.4%–31.6% in FA and 6.2%–8.2% in BA. In the form of needle crystallites, mullite is produced from the

crystallization of melted clay minerals from its coal at high-temperature (Hower 2012; Dai et al. 2010).

#### (4) Fe-oxide minerals.

As for Fe-oxide minerals, the characterization is based on the brightness of the mineral with reddish color under the microscope. Fe-oxide minerals content in FA sample varies from 8.4% to 14.2% and 8.5%–16.4% in BA samples. Fe-oxide minerals in all FA samples are dominated by hematite (7.7%–19.4%), while magnetite (5.1%–29.6%) was found only in several samples. Fe-oxide minerals in FA and BA were probably derived from pyrite in feed coal. Hematite indicated the coal combustion temperature in power plants is less than 1400 °C (Dai et al. 2010).

#### (5) Spinel.

Spinel in FA and BA is characterized by bright mineral and rounded morphology consisting of dendritic texture (Fig. 8). Spinel content in FA sample varies from 5.8% to 16.7% and 8.5%–15.3% in BA samples. XRD analysis identified spinel in FA as Mg-spinel and Fe-spinel. Mg-spinels (2.9%–16.6%) present in all FA samples while Fe-spinels (18.2%–20.5%) only found in FA-6 and FA-8, see Fig. 9. Spinel in FA and BA was derived from high Fe-coal (Hower 2012). Pyrite in feed coal is the source of Fe elements that composed spinels.

#### (6) K-Feldspar.

XRD analysis shows that K-feldspar is only present in FA-2 and FA-5, ranging from 4.6% to 7.7%.

### 3.4 REY in coal, FA, and BA

The geochemical classification of REY was created by Seredin and Dai (2012), which divided REY into light REY (La, Ce, Pr, Nd, and Sm), medium REY (Eu, Gd, Tb, Dy, and Y), and heavy REY (Ho, Er, Tm, Yb, and Lu). In this study, it was found that the average concentration of REY in coal is 9.2 ppm, lower than the average concentration of coal in the US of about 62.1 ppm and China in the average of 139.9 ppm (Dai et al. 2005).

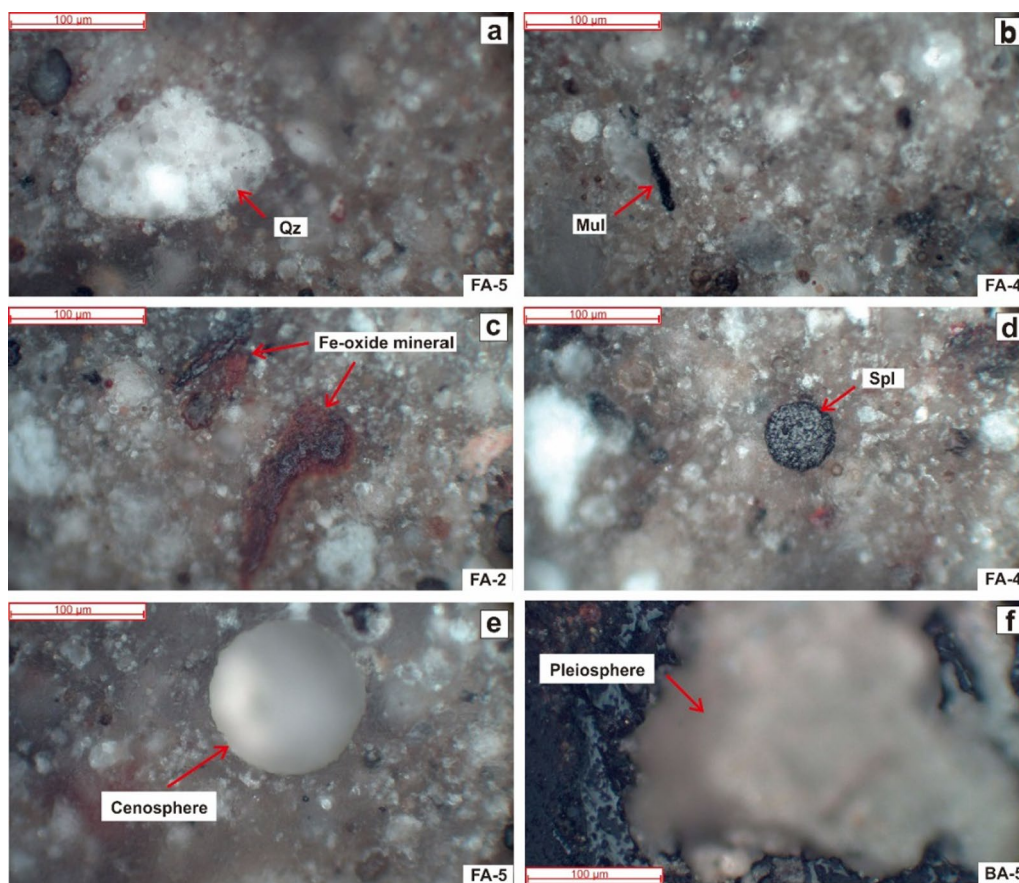


**Fig. 7** Inorganic components of fly ash (FA) and bottom ash (BA). **a** Quartz (Qz); **b** Mullite (Mul); **c** Fe-oxide minerals; **d** Spinel (Spl); **e** Glass cenospheres; and glass **f** Pleiospheres. (All photomicrographs are taken under white light)

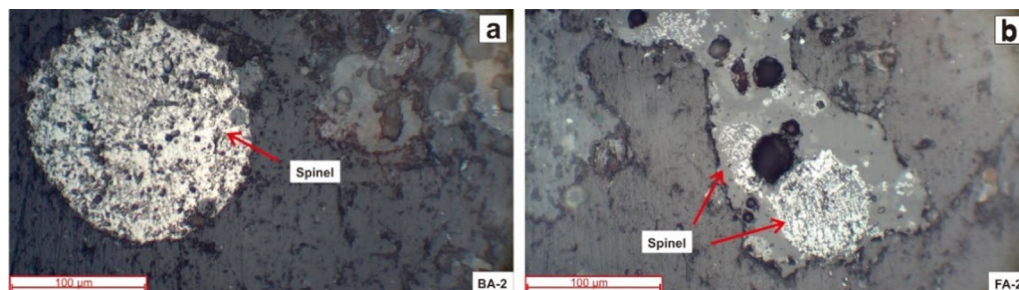


**Fig. 8** Spinel; **a** BA sample; **b** FA sample. (All photomicrographs are taken under white light)

The result of this study showed that individual REY contents in FA are about 10 – 15 times higher than that in coal samples (Fig. 10) because the REY are concentrated in the FA components. Each coal and FA sample's individual REY distribution pattern is relatively similar, but the concentrations are different (“Appendix”). Total REY concentration in coal ranged from 2.10 to 23.67 ppm, with an average of 9.21 ppm. Total REY concentration in FA ranged from 123.14 to 260.38 ppm, with an average of 207.07 ppm.

Total REY concentration in BA ranged from 121.04 to 261.18 ppm, with an average of 171.21 ppm.

Aside from the REY concentration, the abundance of REY concentration, in general, will be converted into REO. The total REO content of FA varies from 148.61 to 313.98 ppm, with an average of 249.70 ppm. This value is higher than the REO content of BA that varies from 146.01 to 314.89 ppm with an average of 231.95 ppm. The total REO content of coal ranges from 2.53 to 28.56 ppm, with



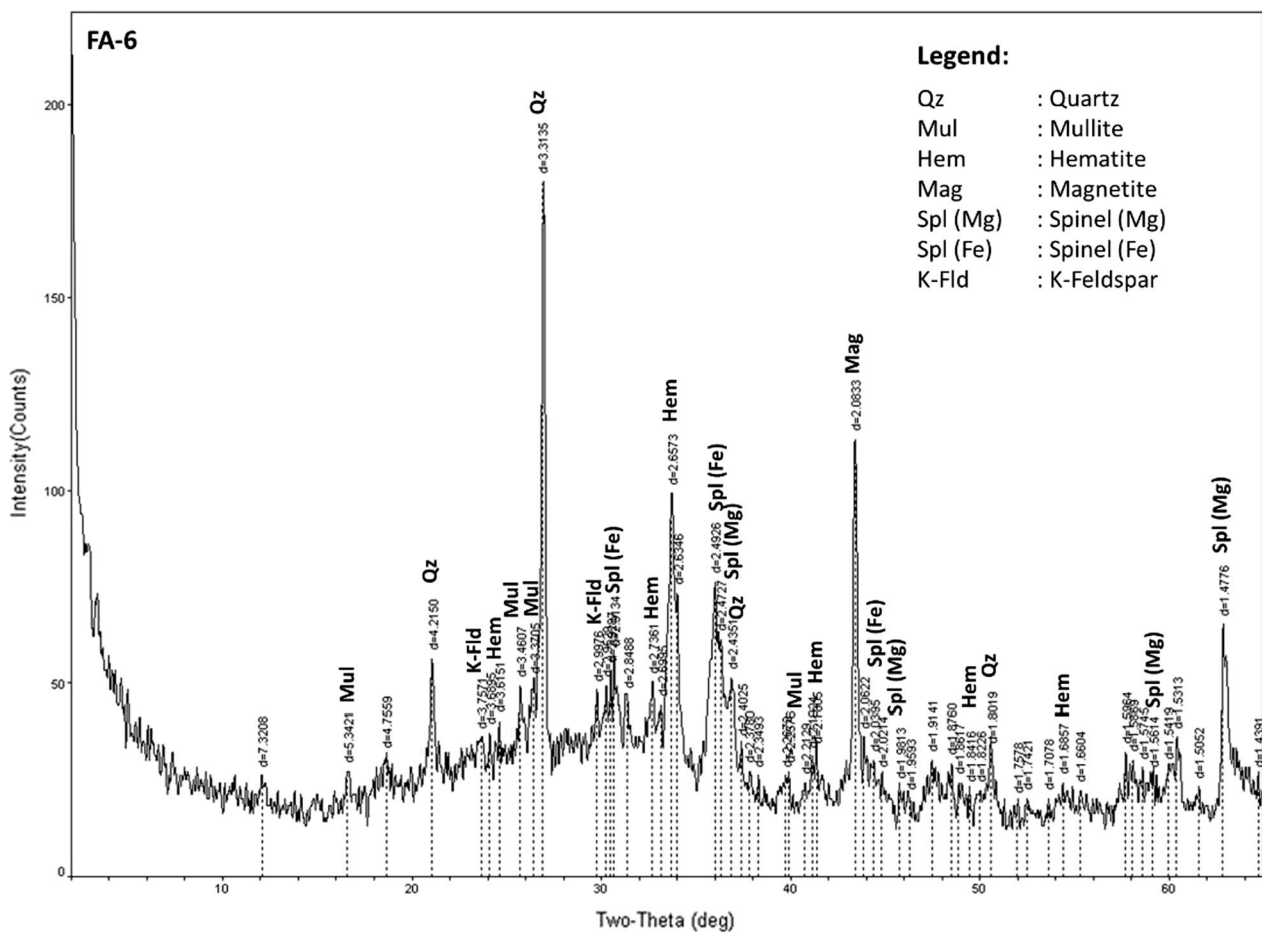


**Fig. 9** X-ray diffraction spectrum for sample fly ash FA 6 showing peaks for the existence of quartz, mullite, k-feldspar, hematite, magnetite, Fe-spinel, and Mg-spinel

an average of 11.10 ppm. REY distribution pattern in FA (Fig. 10) showed HREY enrichment for all samples providing an opportunity to extract all of the REY elements.

- (1) Mode of occurrence of REY in organic components  
SEM–EDX result on the organics showed that the mode of occurrence of Y is negatively correlated with the mode of occurrence of Carbon (Figs. 11 and 12). The mode of occurrence of Carbon (C) and Y represents that Y does not occur in FA's organic components.
- (2) Mode of occurrence of REY in inorganic components  
The mode of occurrence of major elements, including Si and O, is strongly correlated with the mode of occurrence of Y and indicates an overlay area with a high concentration of those elements. Si and O were associated with glass and quartz in FA components. Based on SEM–EDX and petrographic analysis, it is interpreted that high concentrations of Y occur in Glass

(Figs. 13 and 14), including cenospheres and pleiospheres. Spinel in FA consists of Mg, Al, Fe, and O. Mode of occurrence from combinations Mg, Fe, Al, O, and Y elements are positively correlated and made an overlay area that indicates a low concentration of those elements (Fig. 15). Therefore, it can be interpreted that low concentration Y occurs in spinel.

Knowing the mode of occurrence will benefit the leaching technique applied to extract REY from coal fly ash. The correlation of REY with aluminosilicates content in fly ash comprised as the major mineral matrix has been stated by some studies (Kolker et al. 2017; Hower et al. 2018). For this type of sample, alkaline treatment is needed to decompose the aluminosilicate structure before the acid leaching for high recovery of REY (King et al. 2018). It is different from FA with REYs concentrated in Fe- and Ca-enriched fractions (Hower et al. 2018; Hood et al. 2017). Acid leaching

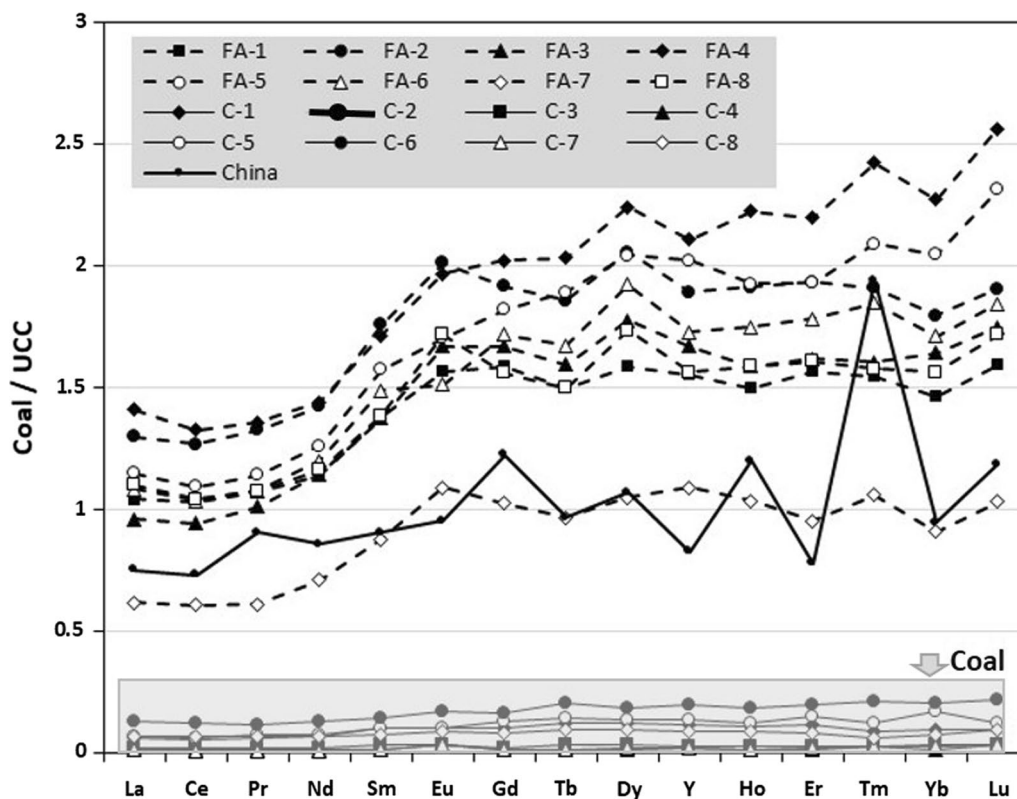


**Fig. 10** Graphic comparison of individual REY contents in coal (C1-C8) and FA (FA1-FA8) samples (normalized to UCC)

will be prone to REY extraction (King et al. 2018; Taggart et al. 2018).

## 4 Conclusions

- (1) From the analysis conducted in this study, it can be concluded that FABA in a coal-fired power plant in Java, Indonesia, consists of inorganic and organic components with different compositions. In the FA, the components include glass (50.7%), quartz (19.7%), mullite (12.6%), Mg-spinel (12.2%), Fe-spinel (9.5%), hematite (9.8%), magnetite (14.4%), K-feldspar (4.9%), and unburned coal (UC) (12.4%). While in BA the components are glass (39.6%), quartz (16.2%), mullite (8.2%), spinel (15.3%), Fe-oxide minerals (16.4%), and UC (19.3%). This composition is aligned with the ash composition in the coal seams.
- (2) Total REY concentration in FA ranged from 123.14 to 260.38 ppm, with an average of 207.07 ppm. The total REO content of FA varies from 148.61 to 313.98 ppm, with an average of 249.70 ppm.
- (3) Based on SEM-EDX and petrographic analysis, we can conclude that Y only occurs in inorganic components of FA. High concentrations of Y are interpreted to occur in amorphous glass, including cenospheres and pleiospheres, while lower concentrations of Y occur in spinel. Mode of occurrence REY in this study could be used as preliminary data to determine the extraction method of REY from Indonesian FA-BA from a coal-fired power plant in Java.

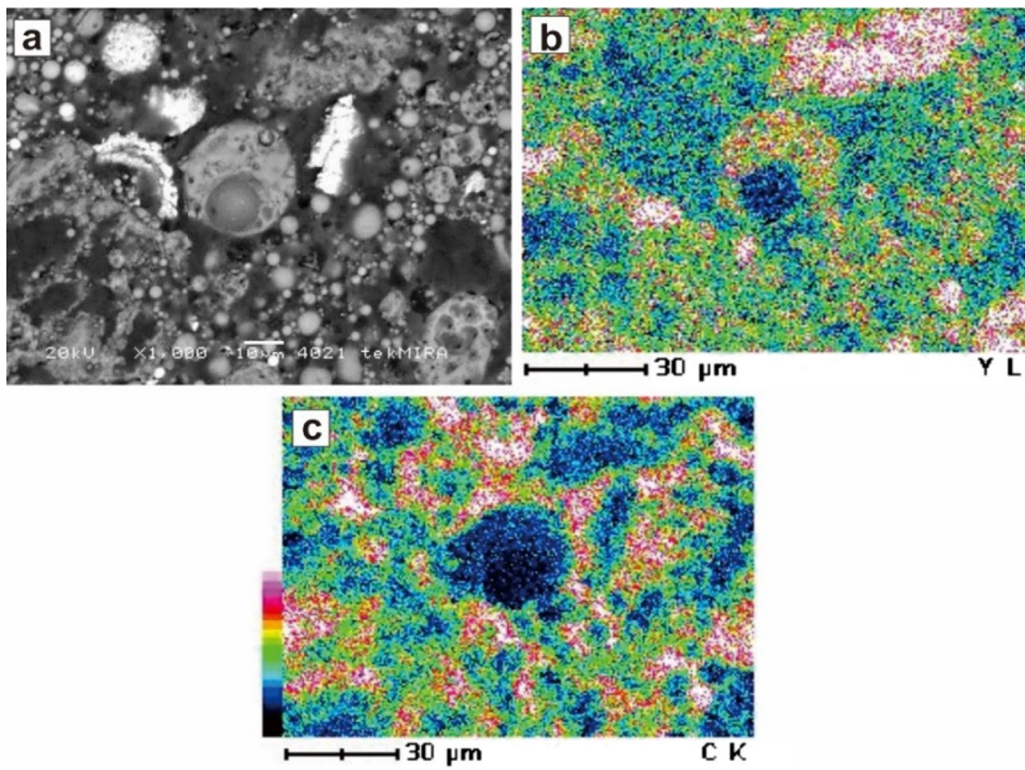


**Fig. 11** Comparison of the mode of occurrence Y and major elements C composed organic components in FA-4 based on SEM-EDX images. **a** backscattered electron image, x1000; elemental mapping shows the distribution of Y (**b**) and the region rich in C (**c**)

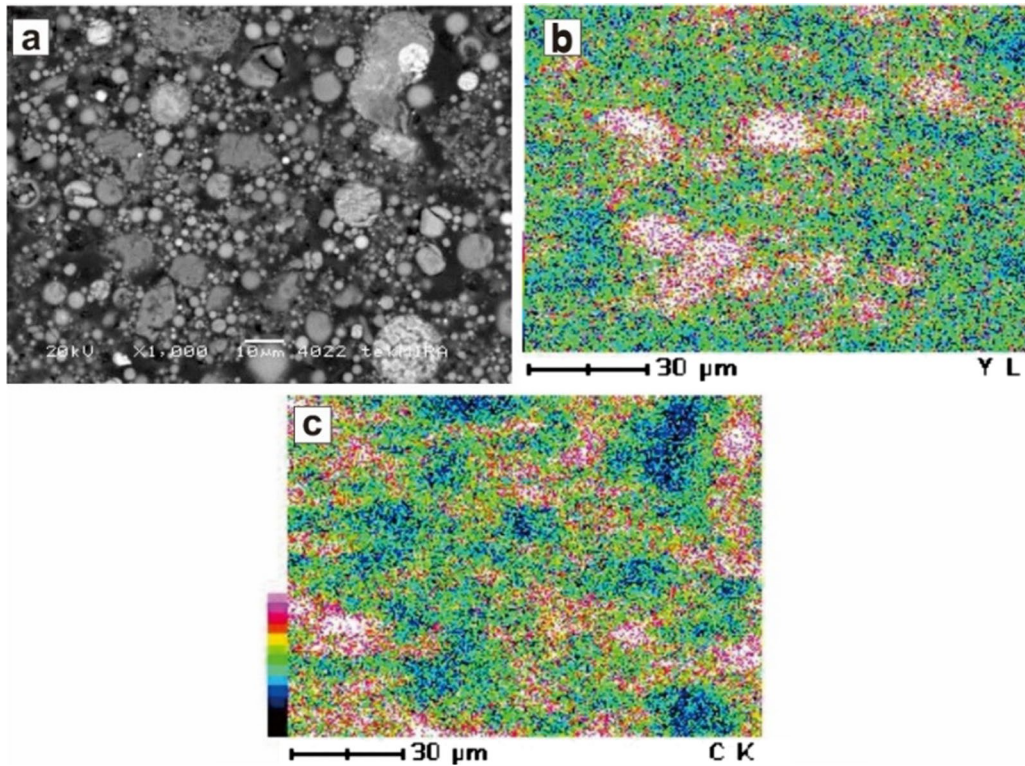


**Fig. 12** Comparison of the mode of occurrence Y and major elements C composed organic components in FA-5 based on SEM-EDX images. **a** Backscattered electron image, x1000; elemental mapping shows the distribution of Y and the region rich in C

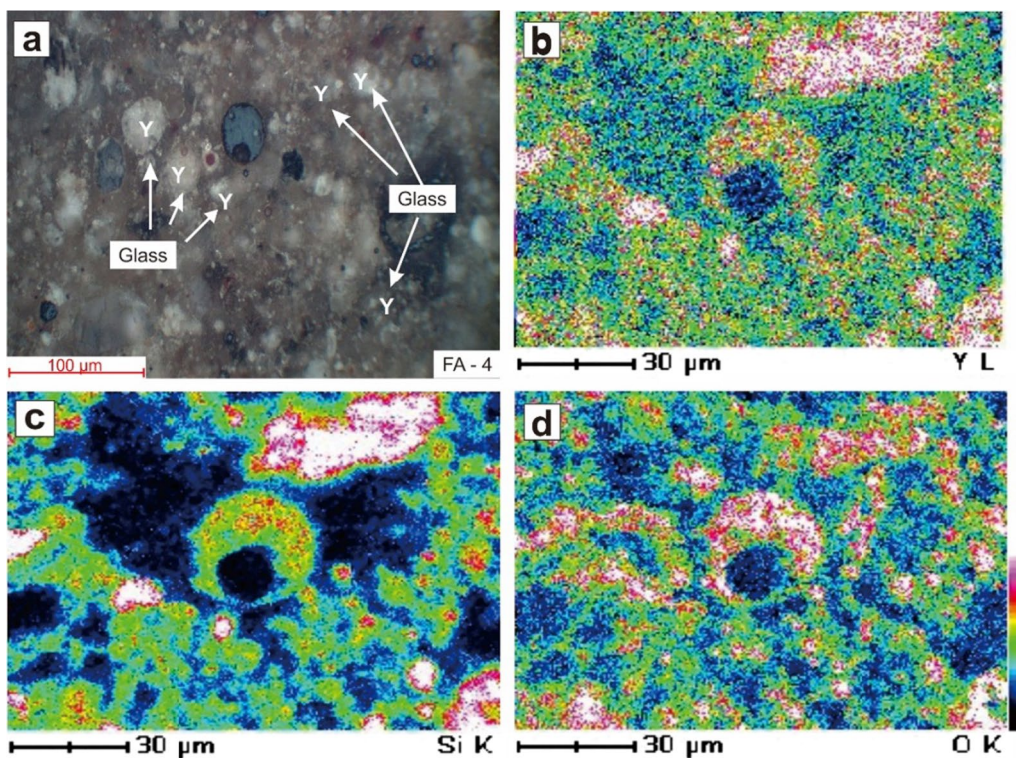


**Fig. 13** Mode of occurrence of Y in Glass (sample FA-4). **a** Optical microscopy of reflected white light; elemental mapping shows the distribution of Y along with the region rich in Si and O

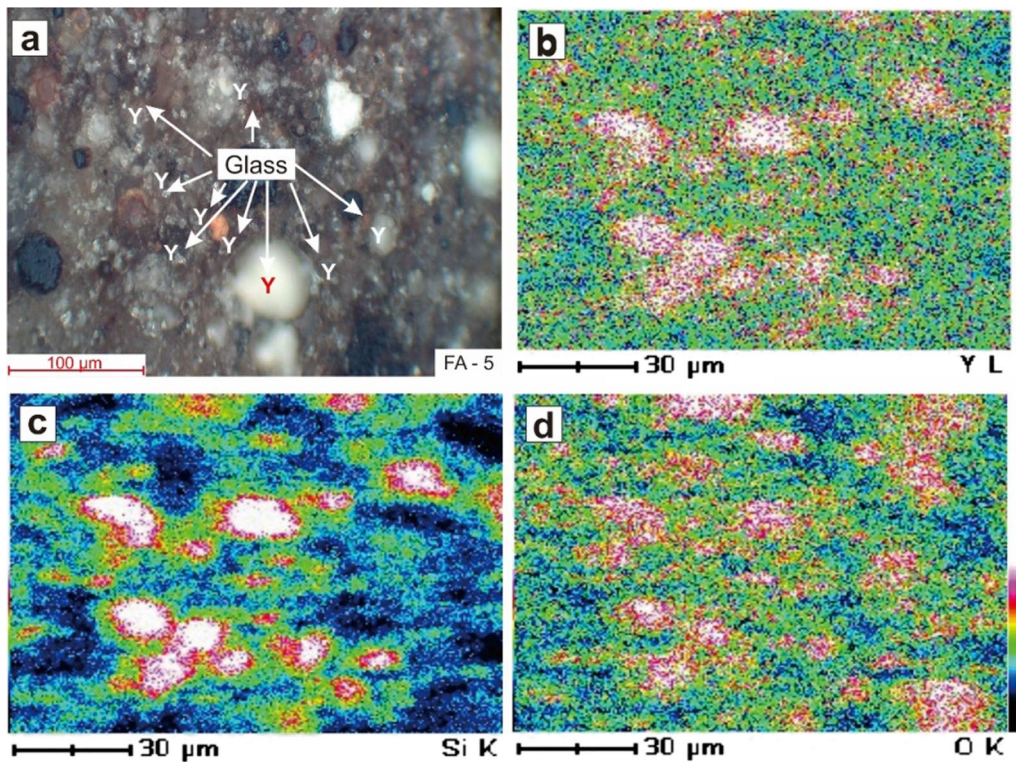


**Fig. 14** Mode of occurrence of Y in Glass (sample FA-5). **a** Optical microscopy of reflected white light; elemental mapping shows the distribution of Y along with the region rich in Si and O

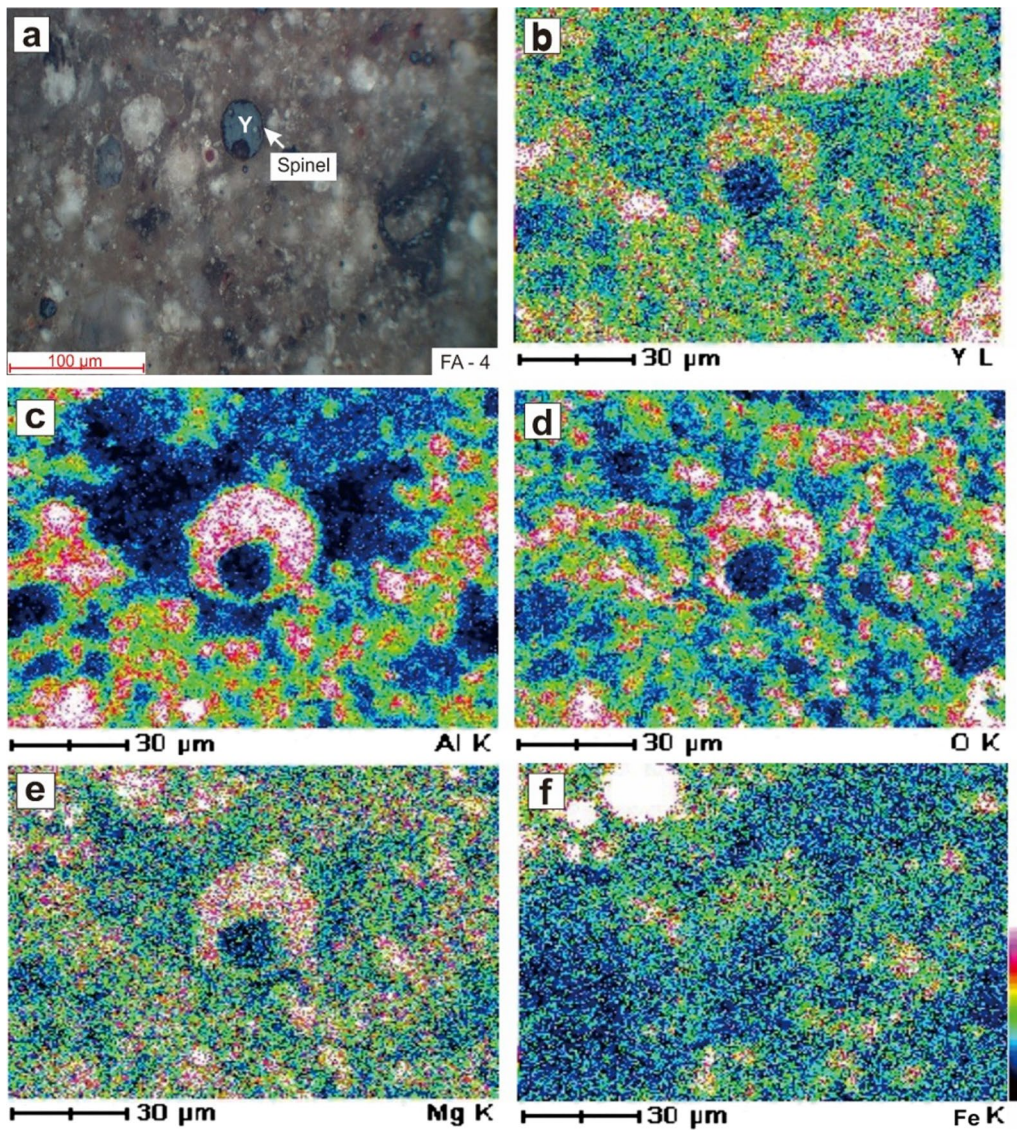


**Fig. 15** Mode of occurrence of Y in spinel (sample FA-4). **a** Optical microscopy reflected of white light; elemental mapping shows the distribution of Y along with the region rich in Al and O, Mg and Fe

## Appendix

Major oxides, LOI, and rare-earth elements analyses of coal, FA, and BA samples from eight coal-fired power plants in northern Java, Indonesia.

Major oxides, LOI, and rare-earth elements analyses of coal, FA, and BA samples from eight coal-fired power plants in northern Java, Indonesia.

Item	Paiton 2			Paiton 1			Pacitan			Tuban			Indramayu			Rembang			Ubjom Paiton			Tanjung Jati		
	C-1	FA-1	BA-1	C-2	FA-2	BA-2	C-3	FA-3	BA-3	C-4	FA-4	BA-4	C-5	FA-5	BA-5	C-6	FA-6	BA-6	C-7	FA-7	BA-7	C-8	FA-8	BA-8
Major Oxides & LOI (%)																								
Si	2.79	53.50	58.20	0.58	50.60	54.00	0.98	41.80	50.40	0.36	50.90	56.40	1.97	42.60	65.70	1.17	35.80	53.90	0.47	34.10	55.80	2.72	49.50	47.00
Al <sub>2</sub>	0.96	20.40	15.10	0.16	23.50	15.50	0.29	16.85	12.60	0.05	28.70	16.85	1.03	20.40	12.30	0.91	16.50	20.40	0.11	9.53	8.43	1.34	22.10	15.70
Fe <sub>2</sub>	0.80	11.25	15.15	2.12	10.90	14.90	0.76	16.85	17.80	0.60	9.04	13.65	0.44	13.75	13.05	0.43	15.95	10.50	0.49	22.00	15.95	0.58	10.55	9.69
Ca	0.23	5.49	4.62	0.56	5.13	4.13	0.77	10.90	9.59	0.96	3.31	6.58	0.12	9.62	3.87	0.85	15.45	8.58	0.35	15.40	9.26	0.23	4.66	3.39
Mg	0.15	3.84	3.45	0.46	3.80	2.74	0.57	7.32	5.44	0.58	2.23	3.19	0.06	6.61	2.34	0.10	10.40	3.28	0.34	14.10	8.06	0.13	2.38	1.96
Na <sub>2</sub>	0.06	0.51	0.33	0.07	0.59	0.33	0.02	0.87	0.44	0.09	0.82	0.28	0.03	0.67	0.46	0.03	0.69	0.39	0.02	0.61	0.48	0.13	2.26	1.18
K <sub>2</sub>	0.09	1.47	0.87	0.02	1.59	0.82	0.03	0.88	0.45	0.02	0.85	0.43	0.04	0.89	0.34	0.01	0.78	0.37	0.01	0.99	0.85	0.10	1.68	1.15
Cr <sub>2</sub>	< 0.01	0.02	0.05	< 0.01	0.02	0.05	< 0.01	0.01	0.02	< 0.01	0.02	0.01	< 0.01	0.01	0.01	< 0.01	0.01	0.01	< 0.01	0.01	0.03	< 0.01	0.02	0.01
Ti	0.04	0.91	0.79	0.01	1.02	0.80	0.02	0.66	0.51	< 0.01	1.04	0.63	0.03	0.79	0.47	0.02	0.62	0.74	0.01	0.52	0.51	0.05	0.87	0.63
Mn	0.01	0.09	0.10	0.01	0.09	0.10	0.01	0.27	0.26	0.01	0.07	0.17	< 0.01	0.21	0.16	0.01	0.24	0.12	0.01	0.37	0.21	< 0.01	0.04	0.04
P <sub>2</sub>	0.01	0.15	0.13	< 0.01	0.16	0.11	< 0.01	0.14	0.11	< 0.01	0.23	0.13	< 0.01	0.12	0.07	< 0.01	0.05	0.04	< 0.01	0.05	0.04	0.01	0.39	0.19
Sr	< 0.01	0.04	0.04	< 0.01	0.04	0.05	< 0.01	0.08	0.08	0.01	0.07	0.07	< 0.01	0.09	0.05	0.01	0.10	0.07	< 0.01	0.11	0.06	0.01	0.17	0.11
Ba	< 0.01	0.09	0.06	< 0.01	0.10	0.06	0.01	0.16	0.10	< 0.01	0.06	0.05	< 0.01	0.15	0.06	< 0.01	0.21	0.07	< 0.01	0.25	0.10	0.01	0.15	0.09
LO	94.20	1.44	2.48	95.30	1.09	4.42	96.10	1.50	0.91	96.90	1.91	0.12	94.90	2.57	1.89	96.20	1.25	1.94	97.60	0.84	1.92	94.30	6.87	16.90
REY (ppm)																								
La	1.90	31.30	25.30	0.50	39.00	26.80	0.60	28.80	22.80	0.50	42.30	27.60	2.10	34.50	20.80	3.90	32.50	41.10	0.50	18.50	18.20	2.10	33.00	2.10
Ce	3.60	66.10	53.40	1.10	81.20	55.40	1.30	60.40	47.00	0.80	84.90	57.50	4.10	70.00	41.50	7.70	66.40	83.60	0.50	39.00	38.60	4.20	66.80	4.20
Pr	0.42	7.60	6.24	0.12	9.43	6.46	0.14	7.19	5.39	0.09	9.65	6.72	0.54	8.11	4.82	0.85	7.64	9.48	0.05	4.34	4.48	0.50	7.64	0.50
Nd	1.70	29.60	24.70	0.50	37.00	26.80	0.50	29.80	21.40	0.30	37.40	27.10	2.00	32.80	19.50	3.40	31.20	38.40	0.20	18.50	18.20	1.80	30.20	1.80
Sm	0.46	6.22	5.50	0.11	7.92	5.56	0.15	6.19	4.91	0.06	7.72	6.25	0.46	7.08	4.29	0.66	6.70	8.24	0.05	3.95	3.84	0.33	6.23	0.33
Eu	0.09	1.38	1.23	0.03	1.77	1.23	0.03	1.47	1.09	0.03	1.73	1.26	0.09	1.50	0.91	0.15	1.33	1.57	0.03	0.96	0.82	0.08	1.51	0.08
Gd	0.38	6.03	5.41	0.08	7.28	5.42	0.09	6.34	4.97	0.05	7.69	6.09	0.50	6.92	4.09	0.63	6.53	8.31	0.06	3.90	3.72	0.31	5.93	0.31
Tb	0.08	0.96	0.85	0.02	1.19	0.86	0.02	1.02	0.80	0.01	1.30	1.00	0.09	1.21	0.72	0.13	1.07	1.31	0.01	0.62	0.60	0.06	0.96	0.06
Dy	0.44	5.56	5.31	0.06	7.20	5.50	0.11	6.21	4.98	0.05	7.84	6.37	0.49	7.15	4.36	0.65	6.73	8.19	0.07	3.67	3.70	0.34	6.07	0.34
Y	2.50	34.20	30.60	0.50	41.60	32.60	0.60	36.70	31.40	0.50	46.40	38.30	3.00	44.50	26.10	4.40	38.00	47.40	0.50	24.00	22.70	1.90	34.40	1.90
Ho	0.09	1.20	1.08	0.01	1.53	1.21	0.02	1.27	1.10	0.01	1.78	1.43	0.10	1.54	0.89	0.15	1.40	1.81	0.01	0.83	0.81	0.07	1.27	0.07
Er	0.27	3.60	3.23	0.06	4.45	3.56	0.06	3.72	3.03	0.03	5.05	4.03	0.34	4.44	2.77	0.46	4.10	5.35	0.04	2.19	2.37	0.19	3.70	0.19
Tm	0.03	0.51	0.48	0.01	0.63	0.51	0.01	0.53	0.50	0.01	0.80	0.66	0.04	0.69	0.39	0.07	0.61	0.80	0.01	0.35	0.36	0.02	0.52	0.02
Yb	0.21	3.22	2.82	0.03	3.95	3.07	0.07	3.61	3.11	0.03	5.00	4.15	0.38	4.50	2.77	0.45	3.76	4.83	0.06	2.00	2.29	0.16	3.44	0.16
Lu	0.03	0.51	0.47	0.01	0.61	0.49	0.01	0.56	0.51	0.01	0.82	0.66	0.04	0.74	0.44	0.07	0.59	0.79	0.01	0.33	0.35	0.03	0.55	0.03
ΣR	12.20	197.9	166.6	3.14	244.7	175.47	3.71	193.81	152.99	2.48	260.38	189.1	14.27	225.6	134.35	23.67	208.5	261.1	2.10	123.1	121.0	12.09	202.2	12.09
LR	66.23	71.12	69.10	74.20	71.31	68.97	72.51	68.30	66.34	70.56	69.89	66.19	64.47	67.57	67.67	69.75	69.26	69.23	61.90	68.45	68.84	73.86	71.15	73.86
HR	33.77	28.88	30.90	25.80	28.69	31.03	27.49	31.70	33.66	29.44	30.11	33.81	35.53	32.43	32.33	30.25	30.74	30.77	38.10	31.55	31.16	26.14	28.85	26.14
CrI	5.08	75.30	65.92	1.17	93.21	70.55	1.32	78.92	62.70	0.92	99.72	78.06	6.01	91.60	54.36	9.19	82.43	102.2	0.85	49.94	48.39	4.37	76.84	4.37

Major oxides, LOI, and rare-earth elements analyses of coal, FA, and BA samples from eight coal-fired power plants in northern Java, Indonesia.

Item	Paiton 2			Paiton 1			Pacitan			Tuban			Indramayu			Rembang			Ubijom Paiton			Tanjung Jati		
	C-1	FA-1	BA-1	C-2	FA-2	BA-2	C-3	FA-3	BA-3	C-4	FA-4	BA-4	C-5	FA-5	BA-5	C-6	FA-6	BA-6	C-7	FA-7	BA-7	C-8	FA-8	BA-8
REY (ppm)																								
Un	3.16	51.15	42.45	0.81	63.63	44.24	0.98	48.52	38.07	0.70	67.36	46.66	3.60	56.61	34.00	6.04	53.37	67.13	0.66	30.69	30.24	3.24	52.80	3.24
Ex	3.96	71.54	58.25	1.16	87.92	60.68	1.41	66.37	52.22	0.86	93.30	64.40	4.66	77.47	45.99	8.44	72.76	91.83	0.59	42.51	42.41	4.48	72.58	4.48
Cri	41.64	38.03	39.56	37.26	38.08	40.21	35.58	40.72	40.98	37.10	38.30	41.28	42.12	40.59	40.46	38.83	39.52	39.14	40.48	40.56	39.98	36.15	38.00	36.15
Ou	1.28	1.05	1.13	1.01	1.06	1.16	0.94	1.19	1.20	1.07	1.07	1.21	1.29	1.18	1.18	1.09	1.13	1.11	1.44	1.17	1.14	0.98	1.06	0.98
ΣR	14.72	238.7	200.9	3.79	295.0	211.59	4.47	233.72	184.69	3.00	313.98	228.2	17.21	272.3	162.06	28.56	251.4	314.9	2.53	148.6	146.0	14.57	243.7	14.57

Legend: Coal (grey), Fly Ash (orange), Bottom Ash (green)

**Acknowledgements** Highly appreciation was conveyed to Publishers dan Publications Board, Universitas Gadjah Mada for partially funding this research.

**Authors' contributions** Dr. Ferian Anggara and Dr. Himawan Tri Bayu Murti are responsible for the research funding, the conception of the study, and manuscript review. While Dea Ayu Anisa Besari and Widya Rosita are responsible for the data collection and manuscript writing. All authors read and approved the final manuscript.

**Funding** The financial support was obtained from Universitas Gadjah Mada with funding number: 828/BPP/2018.

**Availability of data and materials** Data will be shared on request.

**Declarations**

**Consent for publication** Not applicable.

**Competing interests** The arrangement of this manuscript has been assured not to convey any conflict of interest or competing interest among any parties and or authors included in this research work.

**Open Access** This article is licensed under a Creative Commons Attribution 4.0 International License, which permits use, sharing, adaptation, distribution and reproduction in any medium or format, as long as you give appropriate credit to the original author(s) and the source, provide a link to the Creative Commons licence, and indicate if changes were made. The images or other third party material in this article are included in the article's Creative Commons licence, unless indicated otherwise in a credit line to the material. If material is not included in the article's Creative Commons licence and your intended use is not permitted by statutory regulation or exceeds the permitted use, you will

need to obtain permission directly from the copyright holder. To view a copy of this licence, visit <http://creativecommons.org/licenses/by/4.0/>.

**References**

Anggara F, Amijaya DH, Harijoko A, Tambaria TN, Sahri AA, Asa ZAN (2018) Rare earth element and yttrium content of coal in the Banko coalfield, South Sumatra Basin, Indonesia: contributions from tonstein layers. *Int J Coal Geol* 196:159–172

Anggara F, Cikasimi M, Rahmat B, Wibisono SA, Susilawati R (2019) Karakteristik dan genesa pengayaan unsur-unsur tanah jarang pada batubara Lapangan Batubara Muara Tiga Besar Utara, Tanjung Enim, Cekungan Sumatera Selatan. *Buletin Sumber Daya Geologi* 14(3):189–212

Anggara F, Petrus HTBM, Patria AA, Bangun AS (2020) Preliminary study of rare earth element and yttrium (REY) content of coal in Sangatta Coalfield, East Kalimantan, Indonesia. *Indonesian J Geosci* 7(3):301–314

ASTM D2799-05a (2005) Standard test method for microscopical determination of the maceral composition of coal. ASTM International, USA

ASTM D-3174 (2015) Standard test method for ash in the analysis samples of coal and coke from coal. ASTM International, USA

Bashkin VN, Wongyai K (2002) Environmental fluxes of arsenic from lignite mining and power generation in northern Thailand. *Environ Geol* 41(8):883–888

Besari DAA (2018) Komponen penyusun dan model keterdapatn rare earth elements and yttrium (REY) pada fly ash dan bottom ash. Undergraduate thesis. Gadjah Mada University, unpublished

Blissett RS, Smalley N, Rowson NA (2014) An investigation into six coal fly ashes from United Kingdom and Poland to evaluate rare earth element content. *Fuel* 119:236–239

- Dai S, Finkelman RB (2018) Coal as a promising source of critical elements: progress and future prospects. *Int J Coal Geol* 186:155–164. <https://doi.org/10.1016/j.coal.2017.06.005>
- Dai S, Ren D, Tang Y, Yue M, Hao L (2005) Concentration and distribution of elements in Late Permian coals from western Guizhou Province, China. *Int J Coal Geol* 61:119–137
- Dai S, Zhao L, Peng S, Chou L, Wang X, Zhang Y, Li D, Sun Y (2010) Abundances and distribution of minerals and elements in high-alumina coal fly ash from the Jungar Power Plant, Inner Mongolia. *Int J Coal Geol* 81:320–332
- Dai S, Jiang Y, Ward CR, Gu L, Seredin VV, Liu H, Zhou D, Wang X, Sun Y, Zou J, Ren D (2012) Mineralogical and geochemical composition of the coal in the Guanbawansu Mine, Inner Mongolia, China: further evidence for the existence of an Al (Ga and REE) ore deposit in the Jungar coalfield. *Int J Coal Geol* 98:10–40
- Duminda ML, Hullenbusch ED, Annachatre AP (2014) Reuse options for coal fired power plant bottom ash and fly ash. *Rev Environ Sci Biotechnol*. <https://doi.org/10.1007/s11157-014-9336-4>
- Hirajima T, Oosako Y, Nonaka M, Petrus H, Sasaki K, Ando T (2008) Recovery of hollow and spherical particles from coal fly ash by wet separation process. *J MMIJ* 124(12):878–884
- Hirajima T, Petrus H, Oosako Y, Nonaka M, Sasaki K, Ando T (2010) Recovery of cenospheres from coal fly ash using a dry separation process: Separation estimation and potential application. *Int J Miner Process* 95(1–4):18–24
- Honaker RQ, Groppo J, Yoon R-H, Luttrell GH, Noble A, Herbst J (2017) Process evaluation and flowsheet development for the recovery of rare earth elements from coal and associated by products. *Miner Metall Process* 34:107–115
- Hood MM, Taggart RK, Smith RC, Hsu-Kim H, Henke KR, Graham UM, Groppo JG, Unrine JM, Hower JC (2017) Rare earth element distribution in fly ash derived from the Fire Clay coal, Kentucky. *CCGP* 9(1):22–33
- Hower JC (2012) Petrographic examination of coal-combustion fly ash. *Int J Coal Geol* 92:90–97
- Hower JC, Groppo JG, Graham UM, Ward CR, Kostova IJ, Maroto-Valer MM, Dai S (2017) Coal-derived unburned carbons in fly ash: a review. *Int J Coal Geol* 179:11–27
- Hower JC, Qian D, Briot NJ, Henke KR, Hood MM, Taggart RK, Hsu-Kim H (2018) Rare earth element associations in the Kentucky State University stoker ash. *Int J Coal Geol* 189:75–82
- ICCP (2001) The new inertinite classification (ICCP system 1994). *Fuel* 80(4):459–471
- King JF, Taggart RK, Smith RC, Hower JC, Hsu-Kim H (2018) Aqueous acid and alkaline extraction of rare earth elements from coal combustion ash. *Int J Coal Geol* 195:75–83
- Kolker A, Scott C, Hower JC, Vazquez JA, Lopano CL, Dai S (2017) Distribution of rare earth elements in coal combustion fly ash, determined by SHRIMP-RG ion microprobe. *Int J Coal Geol* 184:1–10
- Laudal DA, Benson SA, Addleman RS, Palo D (2018) Leaching behavior of rare earth elements in Fort Union lignite coals of North America. *Int J Coal Geol* 191:112–124
- Manurung H, Rosita W, Petrus HTBM, Bendiyasa IM (2020) Amorphous silicate decomposition from non-magnetic coal fly ash using sodium hydroxide. *IOP Conf Ser Mater Sci Eng* 742(1):012041
- Pecht MG, Kaczmarek RE, Song X, Hazelwood DA, Kavetsky RA, Anand DK (2012) Rare earth materials: insights and concerns. CECD, New York
- Petrus H, Hirajima T, Oosako Y, Nonaka M, Sasaki K, Ando T (2011) Performance of dry-separation processes in the recovery of cenospheres from fly ash and their implementation in a recovery unit. *Int J Miner Process* 98(1–2):15–23
- Pickel W, Kus J, Flores D, Kalaitzidis S, Christanis K, Cardott BJ, Misz-Kennan M, Rodrigues S, Hentschel A, Hamor-Vido M, Crosdale P (2017) Classification of liptinite-ICCP system 1994. *Int J Coal Geol* 169:40–61
- Prihutami P, Prasetya A, Sediawan WB, Petrus HTBM, Anggara F (2021) Study on rare earth elements leaching from magnetic coal fly ash by citric acid. *J Sust Metall* (in press)
- Rybak A, Rybak A (2021) Characteristics of some selected methods of rare earth elements recovery from coal fly ashes. *Metals* 11(1):142
- Seredin VV, Dai S (2012) Coal deposits as potential alternative sources for lanthanides and yttrium. *Int J Coal Geol* 94:67–93
- Sýkorová I, Pickel W, Christanis K, Wolf M, Taylor GH, Flores D (2005) Classification of huminite—ICCP system 1994. *Int Coal Geol* 62(1–2):85–106
- Taggart RK, Hower JC, Hsu-Kim H (2018) Effects of roasting additives and leaching parameters on the extraction of rare earth elements from coal fly ash. *Int J Coal Geol* 196:106–114
- Yao ZT, Ji XS, Sarker PK, Tang JH, Ge LQ, Xia MS, Xi YQ (2015) A comprehensive review on the applications of coal fly ash. *Earth Sci Rev* 141:105–121. <https://doi.org/10.1016/j.earscirev.2014.11.016>
- Zhang W, Noble A (2020) Mineralogy characterization and recovery of rare earth elements from the roof and floor materials of the Guxu coalfield. *Fuel* 270:117533
- Zhang W, Yang X, Honaker RQ (2018) Association characteristic study and preliminary recovery investigation of rare earth elements from Fire Clay seam coal middlings. *Fuel* 215:551–560
- Zhang W, Noble A, Yang X, Honaker R (2020) A comprehensive review of rare earth elements recovery from coal-related materials. *Minerals* 10(5):451